COBEM 2021 26th International Congress of Mechanical Engineering
November 22-26, 2021, Virtual Congress, Brazil

COB-2021-1624-ANALYTICAL STUDY OF ROTOR-STATOR RUBBING PHENOMENON

Tamer El-Sayed[a,b,c]
Heba El-Mongy [a,b]
a) Department of Mechanical Design, Faculty of Engineering, Mataria, Helwan University, P.O. Box 11718, Helmeiat-Elzaton, Cairo, Egypt
b) Centre for Applied Dynamics Research, School of Engineering, University of Aberdeen, Aberdeen, AB24 3UE, UK
c) School of Engineering, University of Hertfordshire, hosted by GAF, *R5 New Garden city, New Capital*, Egypt.
tamer.el-sayed@abdn.ac.uk , heba.el-mongy@abdn.ac.uk
Vahid Vaziri
Centre for Applied Dynamics Research, School of Engineering, University of Aberdeen, Aberdeen, AB24 3UE, UK
vahid.vaziri@abdn.ac.uk
Marian Wiercigroch
Centre for Applied Dynamics Research, School of Engineering, University of Aberdeen, Aberdeen, AB24 3UE, UK
m.wiercigroch@abdn.ac.uk

Abstract. *Rotor-stator rubbing is an intriguing dynamic phenomenon and can cause dangerous effects that may lead to machinery failure, hence, it is of fundamental and practical importance to investigate it. In this study, the established approximate analytical solution to the problem of rotor-stator rubbing is extended to include the Coulomb friction between the rotor and stator. There are two sources of non-smoothness in the investigated problem, where the first is related to the switching between contact and non-contact regimes. The second non-smoothness relates to friction during contact and depends on the change in the direction of the relative velocity between the rotor and stator. The governing equations of motion are strongly nonlinear due to the nonlinear contact forces. The analytical solutions for the individual contact and noncontact regimes are obtained then both solutions are coupled together at the switching interface by precisely evaluating the switching instances. These instances represent the end time for the previous state and the initial time for the new state where switching occurs. Moreover, the relative velocity between the rotor and stator while in contact is monitored to adjust the direction of the tangential contact forces. The results of both the individual contact and noncontact models, and the complete analytical model are verified with the numerical methods based on direct integrations methods. The time response results show that both the numerical and analytical solutions are matched in case of periodic and quasi-periodic responses.*

Keywords: *Rotordynamics, Rotor-stator rubbing, Analytical solution, piecewise smooth, Coulomb friction.*

1. INTRODUCTION

The importance of rotor-stator rubbing in the industry leads to hundreds of experimental and theoretical research studies that deal with this phenomenon. A comprehensive review on rotor-stator rubbing can be found in (Jacquet-Richardet et al., 2013; Prabith and Krishna, 2020). The theoretical models for rotor-stator rubbing may be divided into low dimensional models (Hong et al., 2019; Behzad and Alvandi, 2020; Yang et al., 2021; Feng and Zhang, 2002), continuous system models (Zhang et al., 2021; Phadatare and Pratiher, 2021; Huang et al., 2011; Ma et al., 2015a) or finite element models (Hao et al., 2021; Yu et al., 2021; Liu et al., 2020; Chen et al., 2017; Ma et al., 2015b). Most of the literature is based on low dimensional models as they are relatively simple, which allows for comprehensive analysis of the models and their parameters. In addition, an analytical solution may be derived from such low dimensional models.

Pavlovskaia et al. (2004) introduced a model for the contact between the rotor and preloaded snubber ring. In this model, the snubber ring centre is not fixed and the location after intermittent contact is obtained using the principle of minimum elastic energy. Karpenko et al. (2006) introduced an experimental verification to the model introduced by Pavlovskaia et al. (2004). The results of experimental and theoretical studies are in good correlation to each other. Qin et al. (2008) investigated the grazing bifurcation in the response of rotor-stator rubbing. The rotor model is obtained using the transfer matrix method. The results showed that the response could go to chaos from periodic under grazing bifurcation. Chávez and Wiercigroch (2013) investigated the complex dynamics of intermittent contact between the Jeffcott rotor with bearing clearance. The study was based on path following and detection of periodic trajectories and their bifurcations using TC-HAT software which is a toolbox of AUTO 97. Páez Chávez et al. (2015) investigated a mathematical model for rotor contact with a snubber ring which is isotopically supported. The model is validated with experimental results. The results show that the theoretical model is effective in predicting experimental results at lower frequencies. Wang et al. (2020) investigated the four-dimensional piecewise smooth rotor-stator rubbing system. Their results introduced a deep explanation to the self-excited dry friction. Srivastava et al. (2021) investigated the effect of involving a smoothening function in the rotor rub model. They introduced the benefits of such a model in reducing the computational time. Praveen Krishna and Padmanabhan (2017) investigated the rotor-stator rubbing theoretically and experimentally. The theoretical model is done using harmonic balance method and time variational method. The experimental results are used to validate the proposed model. Yu and Chen (2021) used a combination between harmonic balance method and trust region methods to obtain the rotor stator rub model solution. Hong et al. (2018) investigated theoretically and experimentally the effect of non-smoothness due to rotor stator contact on the system response. The theoretical model is based on finite element modelling. Their results show that the intermittent contact results in a significant increase in the modal frequencies and critical speeds of the rotor.

Karpenko et al. (2002) introduced an approximate analytical solution to the problem of piecewise smooth rotor-stator contact. In this model, the nonlinear contact forces are approximated using first order Taylor's expansion in order to linearize the system equation and to obtain an analytical solution. The contact between the rotor and stator is assumed as frictionless. The model results were very promising in obtaining the system periodic and chaotic responses. Jiang (2009) investigated the rotor-stator rubbing problem based on a low dimensional model. Jiang introduced an analytical solution to the solutions phases, then the solution boundaries in the parameter space were investigated. Shang et al. (2011) extended the work of Jiang (2009) after including the dry friction effects. They concluded that contact stiffness affects the characteristics of dry friction.

The present paper is considered as an extension to the established analytical solution for the piecewise rotor-stator rubbing problem. The Coulomb friction at the contact point is considered in the present model. This increases the complexity of the analytical model. After this introduction, Section 2 introduces the piecewise analytical solutions for the cases of noncontact and contact regimes and the two solutions' coupling. Section 3 introduces the present model results. This includes an evaluation of the contact forces and the system eigenvalues. Then, the effect of introducing the coefficient of friction between the rotor and stator is considered using both the present analytical solution and the direct integration numerical method. Finally, the conclusions section summarizes the main findings.

2. ANALYTICAL MODEL

The physical model of the considered rotor system is assumed be a rotating disc with speed is Ω, having mass m, stiffness and damping of k_r and d_r respectively. The rotor is surrounded by an isotropic circular stator which has a stiffness of k_s. The circular clearance between the rotor and stator is γ as shown in Figure 1. The rotor O_r is the geometrical centre of the rotor, O_s is the geometrical centre of the stator, O_g is the mass centre of the rotor, e is radial distance between the mass center and the geometrical center, and φ_0 is the initial phase angle. R_p is the rotor radius. The x and y coordinates are located at the geometrical centre of the rotor which is assumed constant in this work. The radial position of the geometric centre is $r = \sqrt{x^2 + y^2}$. When the rotor is in contact with the stator, a normal and tangential force components are created

which are F_N and F_T respectively. The coefficient of friction between the rotor and stator is μ. Since the rotor is assumed massless, Jeffcott rotor model can be used to represent the physical model. The equation of motion for the rotor geometrical center can be written in case of $r < \gamma$ as shown in Equation (1). When the rotor contacts the stator i.e. $r > \gamma$, the equation of motion can be written as in Equation (2).

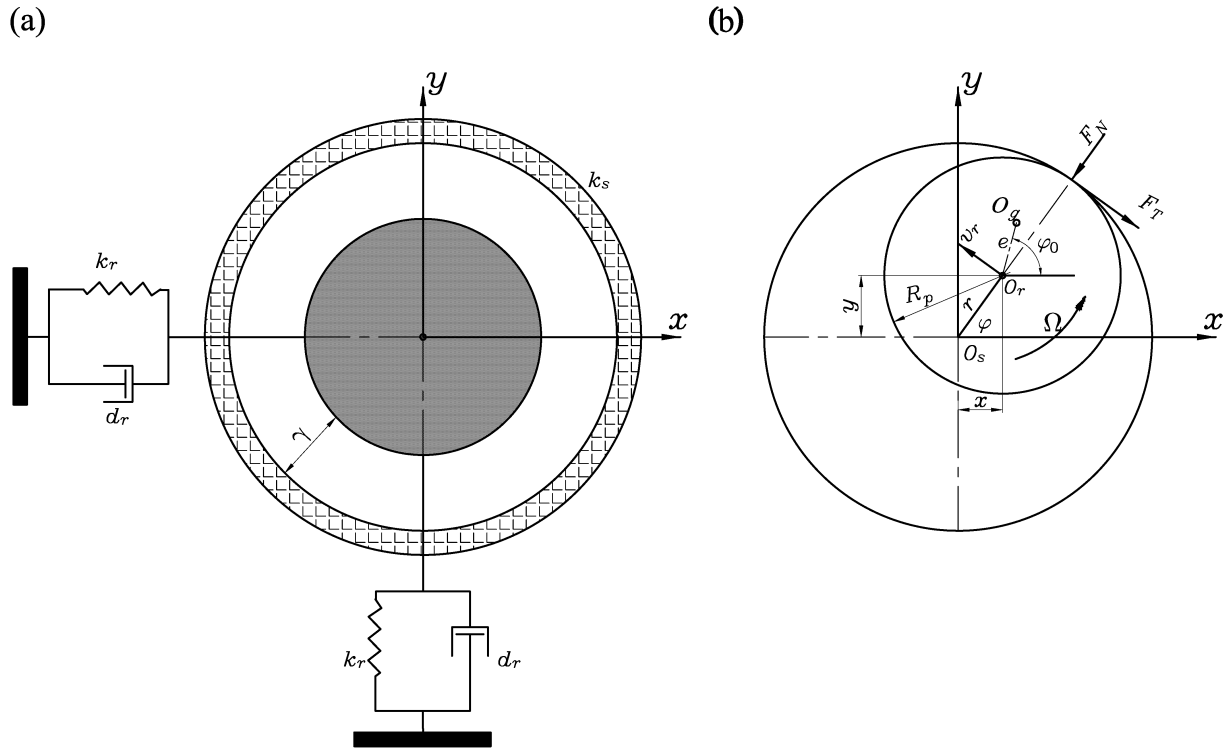

Figure 1 Schematic diagram for rotating disc contact with stiff wall; (a) physical model (b) adopted co-ordinate system and variables.

$$\text{No contact } (r < \gamma): \mathbf{M}\frac{\mathrm{d}^2}{\mathrm{dt}^2}\begin{bmatrix}\mathrm{x}\\ \mathrm{y}\end{bmatrix} + \mathbf{D}\frac{\mathrm{d}}{\mathrm{dt}}\begin{bmatrix}\mathrm{x}\\ \mathrm{y}\end{bmatrix} + \mathbf{K}\begin{bmatrix}\mathrm{x}\\ \mathrm{y}\end{bmatrix} = \mathrm{me}\Omega^2\begin{bmatrix}\cos(\Omega\mathrm{t}+\varphi_0)\\ \sin(\Omega\mathrm{t}+\varphi_0)\end{bmatrix}, \tag{1}$$

$$\text{Contact } (r > \gamma): \mathbf{M}\frac{\mathrm{d}^2}{\mathrm{dt}^2}\begin{bmatrix}\mathrm{x}\\ \mathrm{y}\end{bmatrix} + \mathbf{D}\frac{\mathrm{d}}{\mathrm{dt}}\begin{bmatrix}\mathrm{x}\\ \mathrm{y}\end{bmatrix} + \mathbf{K}\begin{bmatrix}\mathrm{x}\\ \mathrm{y}\end{bmatrix} - \begin{bmatrix}F_x\\ F_y\end{bmatrix} = \mathrm{me}\Omega^2\begin{bmatrix}\cos(\Omega\mathrm{t}+\varphi_0)\\ \sin(\Omega\mathrm{t}+\varphi_0)\end{bmatrix}, \tag{2}$$

where $\mathbf{M} = \begin{bmatrix}m & 0\\ 0 & m\end{bmatrix}$, $\mathbf{D} = \begin{bmatrix}d_r & 0\\ 0 & d_r\end{bmatrix}$ and $\mathbf{K} = \begin{bmatrix}k_r & 0\\ 0 & k_r\end{bmatrix}$.

The vector $[F_x \quad F_y]^T$ represents the nonlinear contact force, where the contact forces in x and y directions:

$$F_x = -F_N(x/r) + F_T(y/r), \qquad F_y = -F_N(y/r) - F_T(x/r),$$

where

$F_N = k_s(r-\gamma)$ and $F_T = \mathrm{sign}(v_r)\,\mu\,F_N = \mu_c\,F_N$,

v_r is the relative velocity between the rotor and stator and can be calculated as:

$$v_r = R_p\omega + \dot{y}(x/r) - \dot{x}(y/r),$$

if $(r-\gamma) > 0$ *and* the relative velocity $v_r \sim 0$, contact stick occurs.

Equations (1-2) can be written in the nondimensional form as:

$$\text{No contact } (\hat{z} < 1): \frac{\mathrm{d}^2}{\mathrm{d}\tau^2}\begin{bmatrix}\hat{x}\\ \hat{y}\end{bmatrix} + 2\nu\frac{\mathrm{d}}{\mathrm{d}\tau}\begin{bmatrix}\hat{x}\\ \hat{y}\end{bmatrix} + \begin{bmatrix}\hat{x}\\ \hat{y}\end{bmatrix} = \hat{e}\eta^2\begin{bmatrix}\cos(\eta\tau + \varphi_0)\\ \sin(\eta\tau + \varphi_0)\end{bmatrix}, \tag{3}$$

$$\text{Contact } (\hat{z} > 1): \frac{\mathrm{d}^2}{\mathrm{d}\tau^2}\begin{bmatrix}\hat{x}\\ \hat{y}\end{bmatrix} + 2\nu\frac{\mathrm{d}}{\mathrm{d}\tau}\begin{bmatrix}\hat{x}\\ \hat{y}\end{bmatrix} + \begin{bmatrix}\hat{x}\\ \hat{y}\end{bmatrix} - \begin{bmatrix}\hat{F}_x\\ \hat{F}_y\end{bmatrix} = \hat{e}\eta^2\begin{bmatrix}\cos(\eta\tau + \varphi_0)\\ \sin(\eta\tau + \varphi_0)\end{bmatrix}, \tag{4}$$

where

$\omega = \sqrt{\frac{k_r}{m}}, \tau = \omega t, ' = \frac{d}{d\tau}, \nu = \frac{d_r}{2\omega m}, \eta = \frac{\Omega}{\omega}, \ \hat{z} = (\hat{x}^2 + \hat{y}^2)^{1/2},$
$K = \frac{k_s}{k_r}$, and $\hat{x} = \frac{x}{\gamma}, \hat{y} = \frac{y}{\gamma}, \hat{e} = \frac{e}{\gamma}.$

The dimensionless nonlinear contact forces can be further expanded as:

$$\hat{F}_x = \frac{F_x}{k_1\gamma} = K\hat{f}_x = +K\,\hat{x}\left(1 - \frac{1}{\hat{z}}\right) - K\,\mu_c\hat{y}\left(1 - \frac{1}{\hat{z}}\right) = +K\hat{f}_{1x}(\hat{x},\hat{y}) - K\mu_c\hat{f}_{2x}(\hat{x},\hat{y}), \tag{5}$$

$$\hat{F}_y = \frac{F_y}{k_1\gamma} = K\hat{f}_y = +K\,\hat{y}\left(1 - \frac{1}{\hat{z}}\right) + K\,\mu_c\hat{x}\left(1 - \frac{1}{\hat{z}}\right) = +K\hat{f}_{1y}(\hat{x},\hat{y}) + K\mu_c\hat{f}_{2y}(\hat{x},\hat{y}), \tag{6}$$

where $\hat{f}_{1x} = \hat{f}_{2y} = \hat{x}\left(1 - \frac{1}{\hat{z}}\right)$ and $\hat{f}_{2x} = \hat{f}_{1y} = \hat{y}\left(1 - \frac{1}{\hat{z}}\right)$.

The analytical solution can be constructed from the linear non-contact solution and the contact solution which is nonlinear. The analytical solution for non-contact equation (1) can be written as:

$$\hat{x} = e^{-\nu t}\left(c_1\cos(\beta\,\tau) + c_2\sin(\beta\,\tau)\right) + c_{11}\cos(\eta\,\tau + \varphi_0) + c_{22}\sin(\eta\,\tau + \varphi_0), \tag{7}$$

$$\hat{y} = \mathrm{e}^{-\nu\,t}\left(c_3\cos(\beta\,\tau) + c_4\sin(\beta\,\tau)\right) + c_{33}\cos(\eta\,\tau + \varphi_0) + c_{44}\sin(\eta\,\tau + \varphi_0), \tag{8}$$

where $\beta = \sqrt{1 - \nu^2}$. c1-c4 are the transient solution constants and c_{11} - c_{44} are the steady state constants. These constants can be obtained from the initial conditions and steady state solution. $\hat{x}'$and $\hat{y}'$ can be obtained by differentiating $\hat{x}$ and $\hat{y}$ with respect to τ.

The analytical solution for the nonlinear contact Equation (2) is more challenging because of the nonlinear contact forces. To derive an analytical solution, the nonlinear contact forces are linearized then an approximate analytical solution to Equation (2) is introduced. The first order Taylor's expansion is used to approximate the contact forces at the contact point. Applying Taylor's expansion to the contact forces Equations (5-6) in the vicinity of $(\tilde{x}_0, \tilde{y}_0)$ results in:

$$\hat{f}_{1x}|_{\substack{\hat{x}=\tilde{x}_0\\ \hat{y}=\tilde{y}_0}} = \hat{f}_{2y}|_{\substack{\hat{x}=\tilde{x}_0\\ \hat{y}=\tilde{y}_0}} = \tilde{x}_0\left(1 - \frac{1}{\sqrt{\alpha}}\right) + \left(1 - \frac{1}{\sqrt{\alpha}} + \frac{\tilde{x}_0^2}{\alpha^{1.5}}\right)(\hat{x} - \tilde{x}_0) + \frac{\tilde{x}_0\tilde{y}_0}{\alpha^{1.5}}(\hat{y} - \tilde{y}_0), \tag{9}$$

$$\hat{f}_{2x}|_{\substack{\hat{x}=\tilde{x}_0\\ \hat{y}=\tilde{y}_0}} = \hat{f}_{1y}|_{\substack{\hat{x}=\tilde{x}_0\\ \hat{y}=\tilde{y}_0}} = \tilde{y}_0\left(1 - \frac{1}{\sqrt{\alpha}}\right) + \left(1 - \frac{1}{\sqrt{\alpha}} + \frac{\tilde{y}_0^2}{\alpha^{1.5}}\right)(\hat{y} - \tilde{y}_0) + \frac{\tilde{x}_0\tilde{y}_0}{\alpha^{1.5}}(\hat{x} - \tilde{x}_0) \tag{10}$$

where $\alpha = \tilde{x}_0^2 + \tilde{y}_0^2$. Equations (9) and (10) can be simplified as:

$$\hat{f}_{1x}|_{\substack{\hat{x}=\tilde{x}_0\\ \hat{y}=\tilde{y}_0}} = \hat{f}_{2y}|_{\substack{\hat{x}=\tilde{x}_0\\ \hat{y}=\tilde{y}_0}} = A_1\,\hat{x} + B_1\,\hat{y} + D_1 \tag{11}$$

$$\hat{f}_{2x}|_{\substack{\hat{x}=\tilde{x}_0\\ \hat{y}=\tilde{y}_0}} = \hat{f}_{1y}|_{\substack{\hat{x}=\tilde{x}_0\\ \hat{y}=\tilde{y}_0}} = A_2\,\hat{y} + B_2\,\hat{x} + D_2 \tag{12}$$

where

$$A_1 = \left(1 - \frac{1}{\sqrt{\alpha}} + \frac{\tilde{x}_0^2}{\alpha^{1.5}}\right), \qquad B_1 = \frac{\tilde{x}_0\tilde{y}_0}{\alpha^{1.5}}, \qquad D_1 = -\frac{\tilde{x}_0}{\sqrt{\alpha}},$$

$$A_2 = \left(1 - \frac{1}{\sqrt{\alpha}} + \frac{\tilde{y}_0^2}{\alpha^{1.5}}\right), \qquad B_2 = \frac{\tilde{x}_0\tilde{y}_0}{\alpha^{1.5}}, \qquad D_2 = -\frac{\tilde{y}_0}{\sqrt{\alpha}},$$

Now, Equations (5) and (6) can be written as:

$$\hat{f}_x|_{\substack{\hat{x}=\tilde{x}_0 \\ \hat{y}=\tilde{y}_0}} = (A_1 - \mu_c B_2)\,\hat{x} + (B_1 - \mu_c\, A_2)\,\hat{y} + (D_1 - \mu_c D_2)\,, \tag{13}$$

$$\hat{f}_y|_{\substack{\hat{x}=\tilde{x}_0 \\ \hat{y}=\tilde{y}_0}} = (B_2 + \mu_c\, A_1)\,\hat{x} + (A_2 + \mu_c B_1)\,\hat{y} + (D_2 + \mu_c D_1)\,. \tag{14}$$

Finally, the contact equations (4) can now be written as:

$$\text{Contact } (\hat{z} > 1): \frac{\mathrm{d}^2}{\mathrm{d}\tau^2}\begin{bmatrix}\hat{\mathrm{x}}\\ \hat{\mathrm{y}}\end{bmatrix} + 2\nu\frac{\mathrm{d}}{\mathrm{d}\mathrm{t}}\begin{bmatrix}\hat{\mathrm{x}}\\ \hat{\mathrm{y}}\end{bmatrix} + \begin{bmatrix}F_{a1} & F_{b1}\\ F_{a2} & F_{b2}\end{bmatrix}\begin{bmatrix}\hat{\mathrm{x}}\\ \hat{\mathrm{y}}\end{bmatrix} = -\begin{bmatrix}F_{d1}\\ F_{d2}\end{bmatrix} + \hat{\mathrm{e}}\Omega^2\begin{bmatrix}\cos(\eta\tau + \varphi_0)\\ \sin(\eta\tau + \varphi_0)\end{bmatrix},$$

where

$$F_{a1} = \big(1 + K(A_1 - \mu_c B_2)\big), \qquad F_{b1} = K(B_1 - \mu_c\, A_2), \qquad F_{d1} = K(D_1 - \mu_c D_2),$$
$$F_{a2} = \big(1 + K(A_2 + \mu_c B_1)\big), \qquad F_{b2} = K(B_2 + \mu_c\, A_1), \qquad F_{d2} = K(D_2 + \mu_c D_1).$$

The analytical solution in this case can be written as:

$$\hat{x} = e^{-\nu\tau}\,(c_1\cos(\gamma_1\tau) + c_2\sin(\gamma_1\tau) + c_3\cos(\gamma_2\tau) + c_4\sin(\gamma_2\tau)) + c_{11}\cos(\varphi_0 + \eta\,\tau) + c_{22}\sin(\eta\,\tau + \varphi_0) + c_{55}, \tag{15}$$

$$\hat{y} = e^{-\nu t}\,(s_1\,c_1\cos(\gamma_1\,\tau) + s_1\,c_2\sin(\gamma_1\,\tau) + s_2\,c_3\cos(\gamma_2\tau) + s_2\,c_4\sin(\gamma_2\,\tau)) + c_{33}\cos(\eta\,\tau + \varphi_0) + c_{44}\sin(\eta\,\tau + \varphi_0) + c_{66}, \tag{16}$$

where

$$s_1 = \frac{\gamma_1^2 + \nu^2 - F_{a1}}{F_{b1}}\,, \tag{17}$$

$$s_2 = \frac{\gamma_2^2 + \nu^2 - F_{a1}}{F_{b1}}\,. \tag{18}$$

The transient solution constants $c_1 - c_4$ and steady state constants $c_{11} - c_{66}$ can be obtained from the initial conditions and the steady state terms.

Up to this point, we have obtained an analytical solution to the individual cases of contact and noncontact. To reach the complete solution, both solutions need to be coupled. This is accomplished by defining the following f_z function as:

$$\hat{f}_z = \sqrt{\hat{x}(\tau;\tau_0,\tilde{x}_0,\tilde{y}_0,\tilde{x}_0',\tilde{y}_0')^2 + \hat{y}(\tau;\tau_0,\tilde{x}_0,\tilde{y}_0,\tilde{x}_0',\tilde{y}_0')^2} - 1\,. \tag{19}$$

If $\hat{f}_z$ is greater than zero, then the contact solution is initiated and vice-versa. The exact time of switching between the two cases is evaluated using bisection method or spline method. In order to achieve higher accuracy in the evaluation of the nonlinear contact force, the contact point location is updated at each time step. Meanwhile during the times when the rotor is in contact with the stator the relative velocity between the rotor and stator is monitored at each time step to adjust the direction of the tangential contact force.

3. RESULTS AND DISCUSSION

In the present section, the nonlinear contact forces are evaluated at the possible contact points locations using the approximate value based on Taylor's form in Equations (9) and (10) and using the exact analytical form. Then, the eigenvalues at the possible locations are also investigated for selected parameters. Finally, different responses are obtained using the present analytical solution and the results are compared with the system solution based on direct numerical integration methods. The general system parameters considered through the present work are listed in Table 1.

Table 1 Non-dimensional parameters considered in the present analysis

Parameter	Value
Borehole stiffness ratio, K	$17.5 - 17.5e5$
Rotor damping ratio, ν	0.009478
Disc radius ratio, $\hat{R}_p = R_p/\gamma$	46.16
Unbalance eccentricity ratio, $\hat{e} = e/\gamma$	46.16
Rotational speed ratio. $\eta = \Omega/\omega$	0.7818
Coefficient of friction, μ	(0- 0.1)

3.1 Contact forces based on approximate and exact values:

In this section, the nonlinear contact forces obtained using equations (5-6) are compared with the nonlinear contact forces evaluated based on the approximate form equations (9-10). This aims to investigate the effect of nonlinear contact force linearization on the evaluated forces. The nonlinear contact forces are function of the rotor's position, the radial clearance, and the borehole stiffness.

The calculated nonlinear forces are presented for the for the case of $K = 17.6\text{e}3,\ \mu = 0.1$. The rest of system parameters are shown in Table 1. The nonlinear horizontal and vertical forces based on the exact equations are shown in the first column of Figure 2 . Similarly, the approximated forces based on first order Taylor approximation are represented in the second column of Figure 2. It is worth noting that the origin of the Taylor approximation is updated at each location. The difference between the exact and the approximate force is presented in the third column of **Error! Reference source not found.** The results show that the forces evaluated using the first order Taylor expansion are very close to the exact results and the deviation between the exact and approximated forces at all points is less than 1e-10. It is also shown that for $\hat{z} < 1$, the contact forces are equal to zero where noncontact condition prevails.

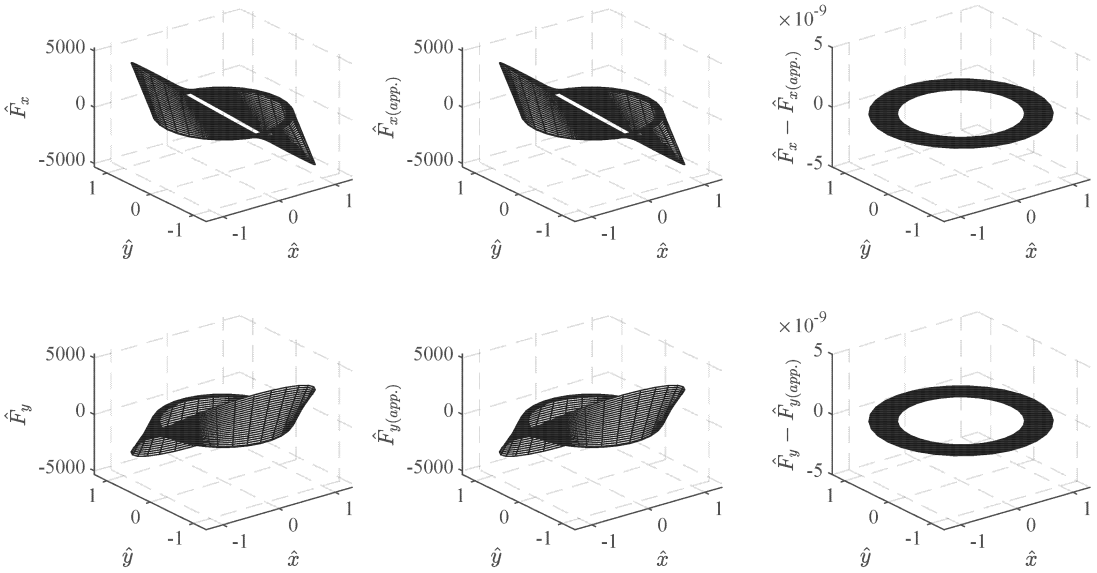

Figure 2 Dimensionless contact force evaluated using exact and approximate forms. The right column represents the difference between forces evaluated using the two methods. ($K = 17.6e3, \mu = 0.1$).

3.2 System response solution

Here the results of the proposed analytical solution are compared with the results of numerical solution for the same problem using direct numerical integration Runge-Kutta ODE45. The system input parameters are shown in Table 1. Six different cases are selected to compare the analytical solution results with the numerical solution results. Figure 3 a-f represent the system flow in case of coefficient of friction $\mu = [0, 0.01, 0.02, 0.03, 0.04, 0.05]$ respectively. The value of relative wall stiffness is selected as $K = 17.6$. The initial conditions are taken as: $\tilde{x}_0 = 0.88544,\ \tilde{x}_0' = 0, \tilde{y}_0 = -0.64312, \tilde{y}_0' = 0$. For all the studied cases, the system responses obtained using both the analytical and numerical solutions are demonstrated in Figure 3. The figure results show that both the analytical and numerical solutions are very close together at $\mu \leq 0.04$. Further increase of the coefficient of friction results in deviation between the two solutions.

Also, the reader can realize that within the present scope of parameters, involving the coefficient of friction results in changing the solution from periodic (Figure 3 a) to quasi-periodic (Figure 3 b-e) then to chaotic (Figure 3 f).

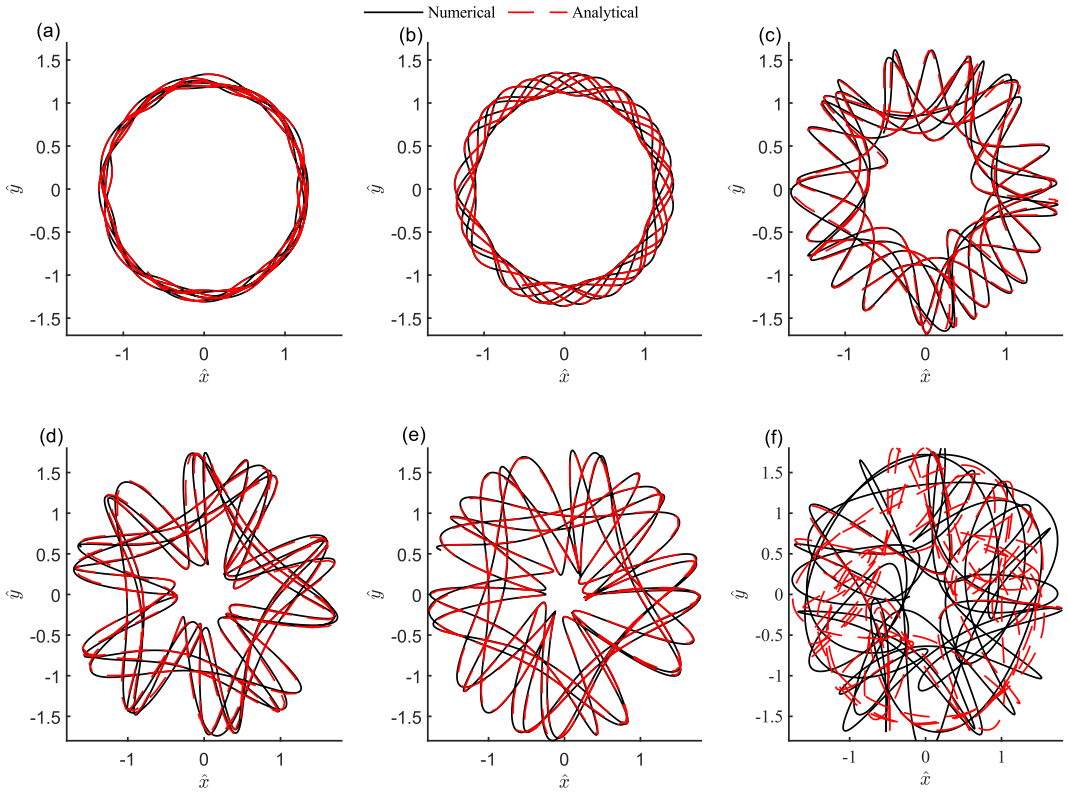

Figure 3 Orbit plots for the nonlinear contact equations using numerical (ODE45) and analytical methods. (a)-(f) [$\mu = 0.0,.01,0.02,0.03,0.04,0.05$] respectively. [$\nu = 0.009478, \eta = 0.7818$, $\hat{e}$=7.52, $\tilde{x}_0 = 0.88544, \tilde{x}_0' = 0, \tilde{y}_0 = -0.8039, \tilde{y}_0' = 0$].

4. CONCLUSIONS

In this work, an approximate analytical solution was obtained for the rotor rubbing problem and the model was applied to the transverse vibrations of the drill-string problem. A derivation of the analytical solution was presented, and the results are compared with the results obtained from direct numerical integration.

The main novelty of this work is in including the frictional effects into the analytical solution for the contact problem and investigating the robustness and validity of the analytical solution for such a highly stiff problem, where brute force numerical simulation can lead to large errors. The present analysis shows that introducing of friction at certain conditions results can result in system instability.

The verification of the analytical solution with the numerical solution shows that both the numerical and analytical solution give the same results in the case of the periodic response and quasi-periodic response. However, by increasing the value of the coefficient of friction, the response becomes chaotic and the numerical and theoretical flows start to deviate.

5. REFERENCES

Behzad M and Alvandi M (2020) Friction-induced backward rub of rotors in non-annular clearances: Experimental observations and numerical analysis. *Tribology International* 152: 106430.

Chávez JP and Wiercigroch M (2013) Bifurcation analysis of periodic orbits of a non-smooth Jeffcott rotor model. *Communications in Nonlinear Science and Numerical Simulation* 18(9): 2571-2580.

Chen L, Qin Z and Chu F (2017) Dynamic characteristics of rub-impact on rotor system with cylindrical shell. *International Journal of Mechanical Sciences* 133: 51-64.

Feng ZC and Zhang X-Z (2002) Rubbing phenomena in rotor–stator contact. *Chaos, Solitons & Fractals* 14(2): 257-267.

Hao L, Han D, Zhao W, Zhao Q and Yang J (2021) Numerical and Experimental Investigation on Axial Rub Impact Dynamic Characteristics of Flexible Rotor Supported by Hybrid Gas Bearings. *Journal of Low Frequency Noise, Vibration and Active Control*. DOI: 10.1177/1461348420986645. 1461348420986645.

Hong J, Yu P, Zhang D and Liang Z (2018) Modal characteristics analysis for a flexible rotor with non-smooth constraint due to intermittent rub-impact. *Chinese Journal of Aeronautics* 31(3): 498-513.

Hong J, Yu P, Zhang D and Ma Y (2019) Nonlinear dynamic analysis using the complex nonlinear modes for a rotor system with an additional constraint due to rub-impact. *Mechanical Systems and Signal Processing* 116: 443-461.

Huang Z, Zhou J, Yang M and Zhang Y (2011) Vibration characteristics of a hydraulic generator unit rotor system with parallel misalignment and rub-impact. *Archive of Applied Mechanics* 81(7): 829-838.

Jacquet-Richardet G, Torkhani M, Cartraud P, Thouverez F, Baranger TN, Herran M, Gibert C, Baguet S, Almeida P and Peletan L (2013) Rotor to stator contacts in turbomachines. Review and application. *Mechanical Systems and Signal Processing* 40(2): 401-420.

Jiang J (2009) Determination of the global responses characteristics of a piecewise smooth dynamical system with contact. *Nonlinear Dynamics* 57(3): 351-361.

Karpenko EV, Wiercigroch M, Pavlovskaia EE and Cartmell MP (2002) Piecewise approximate analytical solutions for a Jeffcott rotor with a snubber ring. *International Journal of Mechanical Sciences* 44(3): 475-488.

Karpenko EV, Wiercigroch M, Pavlovskaia EE and Neilson RD (2006) Experimental verification of Jeffcott rotor model with preloaded snubber ring. *Journal of sound and vibration* 298(4): 907-917.

Liu Y, Li JT, Feng KP, Zhao YL, Yan XX and Ma H (2020) A novel fault diagnosis method for rotor rub-impact based on nonlinear output frequency response functions and stochastic resonance. *Journal of sound and vibration* 481: 115421.

Ma H, Lu Y, Wu Z, Tai X, Li H and Wen B (2015a) A new dynamic model of rotor–blade systems. *Journal of sound and vibration* 357: 168-194.

Ma H, Zhao Q, Zhao X, Han Q and Wen B (2015b) Dynamic characteristics analysis of a rotor–stator system under different rubbing forms. *Applied Mathematical Modelling* 39(8): 2392-2408.

Páez Chávez J, Vaziri Hamaneh V and Wiercigroch M (2015) Modelling and experimental verification of an asymmetric Jeffcott rotor with radial clearance. *Journal of sound and vibration* 334: 86-97.

Pavlovskaia EE, Karpenko EV and Wiercigroch M (2004) Non-linear dynamic interactions of a Jeffcott rotor with preloaded snubber ring. *Journal of sound and vibration* 276(1): 361-379.

Phadatare HP and Pratiher B (2021) Large deflection model for rub-impact analysis in high-speed rotor-bearing system with mass unbalance. *International Journal of Non-Linear Mechanics* 132: 103702.

Prabith K and Krishna IRP (2020) The numerical modeling of rotor–stator rubbing in rotating machinery: a comprehensive review. *Nonlinear Dynamics*. DOI: https://doi.org/10.1007/s11071-020-05832-y. 1-47.

Praveen Krishna IR and Padmanabhan C (2017) Experimental and numerical investigations on rotor–stator rub. *Proceedings of the Institution of Mechanical Engineers, Part C: Journal of Mechanical Engineering Science* 232(18): 3200-3212.

Qin W, Su H and Yang Y (2008) Grazing bifurcation and chaos in response of rubbing rotor. *Chaos, Solitons & Fractals* 37(1): 166-174.

Shang Z, Jiang J and Hong L (2011) The global responses characteristics of a rotor/stator rubbing system with dry friction effects. *Journal of sound and vibration* 330(10): 2150-2160.

Srivastava AK, Tiwari M and Singh A (2021) Identification of rotor-stator rub and dependence of dry whip boundary on rotor parameters. *Mechanical Systems and Signal Processing* 159: 107845.

Wang S, Hong L and Jiang J (2020) Characteristics of stick-slip oscillations in dry friction backward whirl of piecewise smooth rotor/stator rubbing systems. *Mechanical Systems and Signal Processing* 135: 106387.

Yang Y, Tang J, Chen G, Yang Y and Cao D (2021) Rub-Impact Investigation of a Single-Rotor System Considering Coating Effect and Coating Hardness. *Journal of Vibration Engineering & Technologies* 9(3): 491-505.

Yu P and Chen G (2021) Nonlinear modal analysis and its application on prediction of resonance speed for a rotor–stator rubbing system. *Journal of the Brazilian Society of Mechanical Sciences and Engineering* 43(4): 209.

Yu P, Chen G and Li L (2021) Modal analysis strategy and nonlinear dynamic characteristics of complicated aero-engine dual-rotor system with rub-impact. *Chinese Journal of Aeronautics*. DOI: https://doi.org/10.1016/j.cja.2020.10.031.

Zhang J, Zhang L, Ma Z, Wang X, Wu Q and Fan Z (2021) Coupled bending-torsional vibration analysis for rotor-bearing system with rub-impact of hydraulic generating set under both dynamic and static eccentric electromagnetic excitation. *Chaos, Solitons & Fractals* 147: 110960.

6. RESPONSIBILITY NOTICE

The authors are the only responsible for the printed material included in this paper.